

# Crystallization behaviour of poly(*N*-methyldodecano-12-lactam) Part 1. Isothermal crystallization

J. Kratochvíl\*, A. Sikora, J. Baldrian, J. Dybal, R. Puffr

*Institute of Macromolecular Chemistry, Academy of Sciences of the Czech Republic, 162 06 Prague 6, Czech Republic*

Received 4 June 1999; received in revised form 20 January 2000; accepted 7 February 2000

## Abstract

Differential scanning calorimetry (DSC), wide-angle X-ray scattering (WAXS) and Raman spectroscopy have revealed a complex melting/crystallization behaviour of poly(*N*-methyldodecano-12-lactam), MPA. After cooling from the melt to crystallization temperature  $T_c$  of 250–280 K, primary lamellar structure is formed which melts at about 324 K. During later stages of isothermal crystallization, imperfect “fringed” crystallites melting at about  $T_c + 10$  K are formed in the interlamellar space of the primary structure. On heating, additional crystallization of the primary lamellae takes place with an optimum temperature at about 300 K. In the case of isothermal crystallization at  $T_c = 290$  K and higher, the two steps of the primary structure formation combine in a single isothermal step. Under certain conditions an additional endotherm, possibly corresponding to some less-defected “fringed” lamellae, was detected. On further heating, the primary crystallites undergo recrystallization with an optimum temperature at about 327 K. The final higher-ordered structure melts at about 335 K. Melting temperature of the imperfect crystallites shows a strong dependence while that of the highest-melting structure a negligible dependence on  $T_c$ . Within 24 h at 300 K, the MPA sample reaches crystallinity of about 34%. © 2000 Elsevier Science Ltd. All rights reserved.

*Keywords:* *N*-methylated polyamide; Crystallization; Differential scanning calorimetry

## 1. Introduction

Methyl substituents on amide groups of aliphatic polyamides prevent both the formation of hydrogen bridges between chains and a denser packing of methylene units compared with unsubstituted polyamides. Weakening of intermolecular interactions leads to a lower glass-transition temperature, melting temperature, crystallinity, modulus of elasticity, hardness and strength, and to increased toughness, permeability to low-molecular-weight substances and solubility in common solvents. Studies published in literature regarded mainly the structure and properties of polyamides prepared by condensation of diacids with *N*-methylated diamines [1,2]. Polyamides obtained by polymerization of *N*-methyl lactams were studied to a lesser extent [3–6].

Poly(*N*-methyldodecano-12-lactam) (MPA) is known to exhibit a complex melting/crystallization behaviour [3–5]. Such behaviour of semicrystalline polymers is a relatively frequently encountered phenomenon. In the literature, the occurrence of multiple endotherms/exotherms in DSC

thermograms is interpreted in various ways. The cause can lie in the presence of two or more morphological structures in the polymer under study [7,8], the coexistence of lamellae of different thicknesses, i.e. lamellar polymorphism [9]. Quite often is the occurrence of multiple peaks in DSC thermograms associated with perfection of crystalline structures caused by reorganization during annealing and/or partial melting and recrystallization. In these cases, the position of the lower melting endotherm associated with less perfectly ordered structures features a relatively strong dependence on crystallization temperature  $T_c$ , whereas the maximum of the endotherm of recrystallized structures is virtually independent of  $T_c$  [10,11]. Several authors have identified three endotherms in DSC thermograms and associated them with melting of crystalline structures formed by primary crystallization, secondary crystallization and recrystallization [12,13].

Crystallization behaviour of MPA was investigated by Shalaby and co-workers [3–5]. They found a 19% crystallinity of MPA compared with a 40% crystallinity of non-methylated polyamide 12 (PA12). As MPA is unable to form H-bridges, its melting temperature is considerably lower than that of PA12. The crystalline structure of MPA is different from that of PA12. From this point of view, the

\* Corresponding author.

E-mail address: jakr@imc.cas.cz (J. Kratochvíl).

Table 1  
Samples of poly(*N*-methyl dodecano-12-lactam)

	Polymerization		LS	GPC			$T_g$ (K)
	<i>i</i> (mmol/kg)	<i>t</i> (h)	$M_w$	$M_n$	$M_w$	$M_w/M_n$	
MPA 5	292	17	4500	3700	6100	1.66	239.7
MPA 15	93	52	14 900	10 500	22 000	2.10	241.2
MPA 45	31	152	46 700	28 600	59 200	2.07	241.0

authors rather related MPA to a polyethylene-like polymer with methylated amide groups representing chemical defects in a uniform structure. By DSC analysis, the authors [3–5] revealed a multiple-endotherm/exotherm behaviour of MPA and, on the basis of X-ray and DSC analyses, they attributed the complex melting behaviour of this polymer to differences in size and perfection of crystallites and not to polymorphism.

Using a combination of spectroscopic methods (IR, Raman and NMR), it was found that in amorphous MPA an equilibrium exists between *cis* and *trans* conformations of the methylated amide group [6]. In the crystalline phase of semicrystalline MPA, the amide bond is present in the *cis* form and the polymethylene segments contain long *trans* sequences, with a *trans* conformation on the CH<sub>2</sub>–CO bond.

This first part of the study on crystallization/melting behaviour of MPA summarizes the results of DSC characterization of isothermal crystallization completed with data from WAXS and Raman spectroscopic methods.

## 2. Materials and methods

### 2.1. Poly(*N*-methyl dodecano-12-lactam)

The samples of poly(*N*-methyl dodecano-12-lactam), MPA (= methylated polyamide 12), CH<sub>3</sub>–(CH<sub>2</sub>)<sub>11</sub>–CO[N(CH<sub>3</sub>)–(CH<sub>2</sub>)<sub>11</sub>–CO]<sub>*n*</sub>–OH were prepared by acidolytic polymerization of *N*-methyl dodecano-12-lactam [14] followed by extraction with diethyl ether and vacuum drying at 25°C for 24 h and at 45°C for 8 h. Molecular weights were determined by the light scattering (LS) method in dioxane solution and by the gel permeation chromatography (GPC) in tetrahydrofuran. The polymerization parameters (concentration of initiating dodecanoic acid *i* and polymerization time *t* at 260°C), molecular weight parameters and glass transition temperatures  $T_g$  are listed in Table 1.

### 2.2. Differential scanning calorimetry

A Perkin–Elmer DSC 2 apparatus was employed for calorimetric measurements. In later stages, the experiments were performed on a Perkin–Elmer Pyris 1 DSC apparatus. Samples of about 5 mg were closed in aluminium sample pans, the system was flushed with dry nitrogen or helium (Pyris) during the DSC scan. The temperature scales of both

apparatus were calibrated according to the melting points of cyclohexane and indium. The power output scales of DSC 2 and Pyris 1 were calibrated with Al<sub>2</sub>O<sub>3</sub> and indium, respectively.

The as-prepared samples were scanned in the temperature interval 280–360 K at a heating rate HR of 10 K/min. In the enthalpy balance measurements, the as-prepared sample was cooled down at the cooling rate CR = –200 K/min to 100 K, scanned to 360 K (HR = 10 K/min), kept there for 10 min, scanned during cooling to 100 K (CR = –10 K/min) and immediately rescanned to 360 K (HR = 10 K/min).

In the studies of crystallization of MPA at 270 K for different periods of time, the sample was heated at HR of 200 K/min to 360 K, allowed for 10 min, cooled down at CR of –200 K/min to 270 K, and allowed for a specified period of time. The DSC scan was carried out at a HR of 10 K/min.

In the study of the influence of different HR during the DSC scan, the first steps of melting and cooling were the same as above; the sample was then kept at 270 K for 60 min and scanned at different HR in the range of 2–40 K/min.

In the studies of isothermal crystallization at different crystallization temperatures  $T_c$ , MPA samples were melted at 360 K for 10 min, cooled down (CR = –320 K/min) to the respective crystallization temperature  $T_c$  within the range 250–305 K and held at this temperature for 60 min. Then, DSC thermograms were recorded in the temperature range from  $T_c$  to 350 K at a HR of 5 K/min. The melting temperature  $T_m$  and exotherm temperature were taken at the maximum of an endotherm and the minimum of an exotherm, respectively.

In the long-term crystallization experiments, the samples after melting were brought to 300 K and kept at this  $T_c$  for up to one month with the DSC scans being recorded at certain time intervals. In the measurements of  $T_g$ , the as-prepared MPA samples were put into the DSC apparatus, cooled down at CR of 10 K/min to 100 K and scanned at HR of 10 K/min to 300 K.

### 2.3. X-ray measurements

Wide-angle X-ray scattering (WAXS) measurements were performed with an automated, computer-controlled diffractometer HZG/4A (Prazisionsmechanik Freiberg

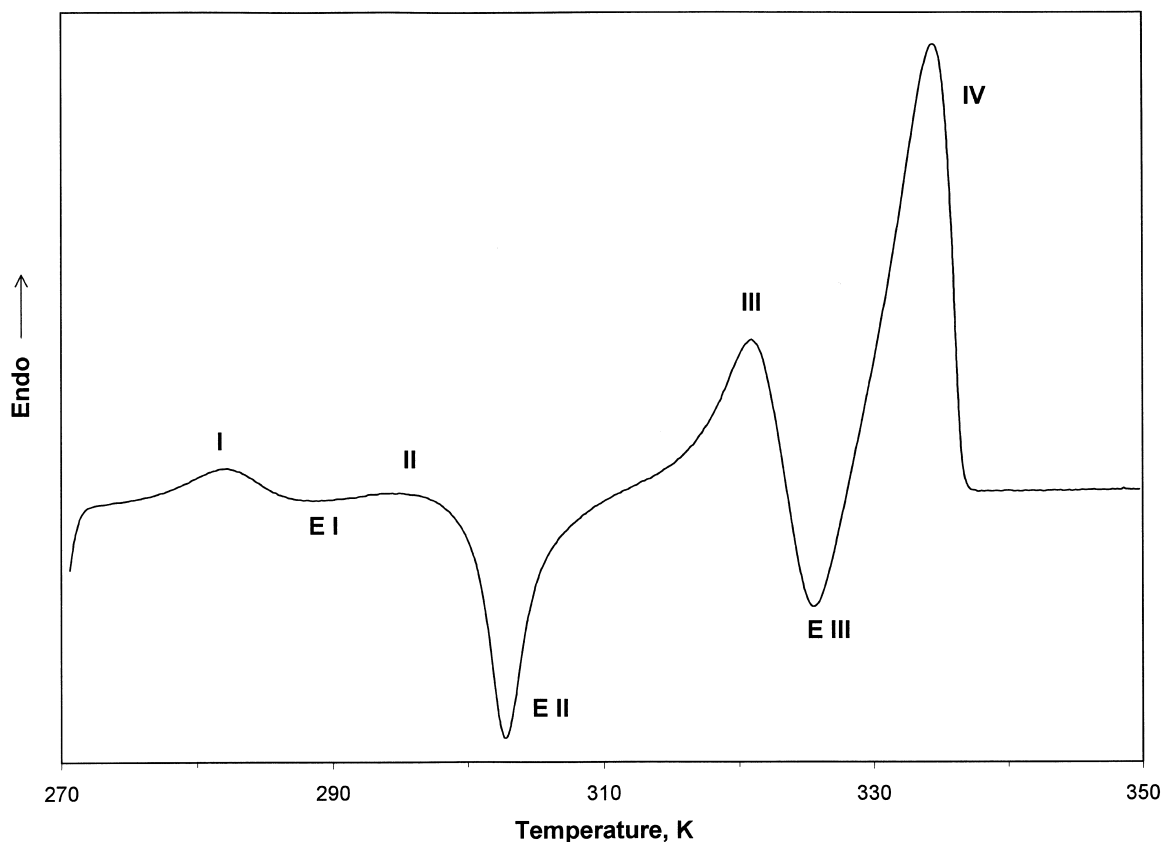


Fig. 1. DSC thermograms of MPA 5 crystallized at 270 K for 60 min. HR = 5 K/min. Roman numerals designate respective endotherms and exotherms referred to in the text.

GmbH, Germany). The CuK $\alpha$  radiation filtered electronically and with a Ni filter was applied. The crystallinities were estimated using WAXS integral intensities diffracted by crystalline and amorphous phases.

#### 2.4. Spectroscopic measurements

Raman spectra were scanned on a Bruker IFS-55 FT-IR spectrometer equipped with a Raman module FRA 106 and the spectra were recorded at a 2 cm<sup>-1</sup> resolution. Samples were excited using a 1064 nm diode-pumped Nd:YAG laser with a power of 100 mW at a sample. The samples were stamped into depressions in aluminium discs where they were kept during the heat treatment. The samples were measured as prepared, then heated under vacuum at 360 K for 10 min, cooled down to room temperature and isothermally crystallized at laboratory temperature for 48 h.

### 3. Results and discussion

Poly(*N*-methyldodecano-12-lactam) shows a complex crystallization/melting behaviour. Fig. 1 presents a typical DSC thermogram of this polymer with the Roman numerals designating respective endotherms and exotherms as they will be referred to in the following text. The main aim of this

study was to identify the processes taking place in MPA that are associated with these endotherms and exotherms.

#### 3.1. As-prepared samples

The DSC thermograms (280–360 K) of the as-prepared samples in Fig. 2 differ considerably depending on molecular weight. All these samples feature a minor broad peak at 310–312 K. The main endotherm of the two higher-molecular-weight samples with the maximum at about 330 K is accompanied by a shoulder peak at about 335 K. In the low-molecular-weight sample (MPA 5), these two endotherms are almost completely separated and show maxima at 327 and 336 K, respectively. Moreover, the latter endotherm is accompanied by another shoulder peak at about 340 K. As it is shown in the second part of this study [15], this behaviour can be explained by the effect of the final annealing temperature (318 K) and molecular weight and/or molecular-weight distribution on recrystallization of the as-prepared samples.

Fig. 3 presents DSC thermograms of sample MPA 5 scanned within the temperature interval 100–360 K (only the interval 200–360 K is shown). The thermogram of the first run (as-prepared sample) shows a weak glass transition at about 240 K and melting of the crystalline portion accompanied by recrystallization. During cooling of the melt, the

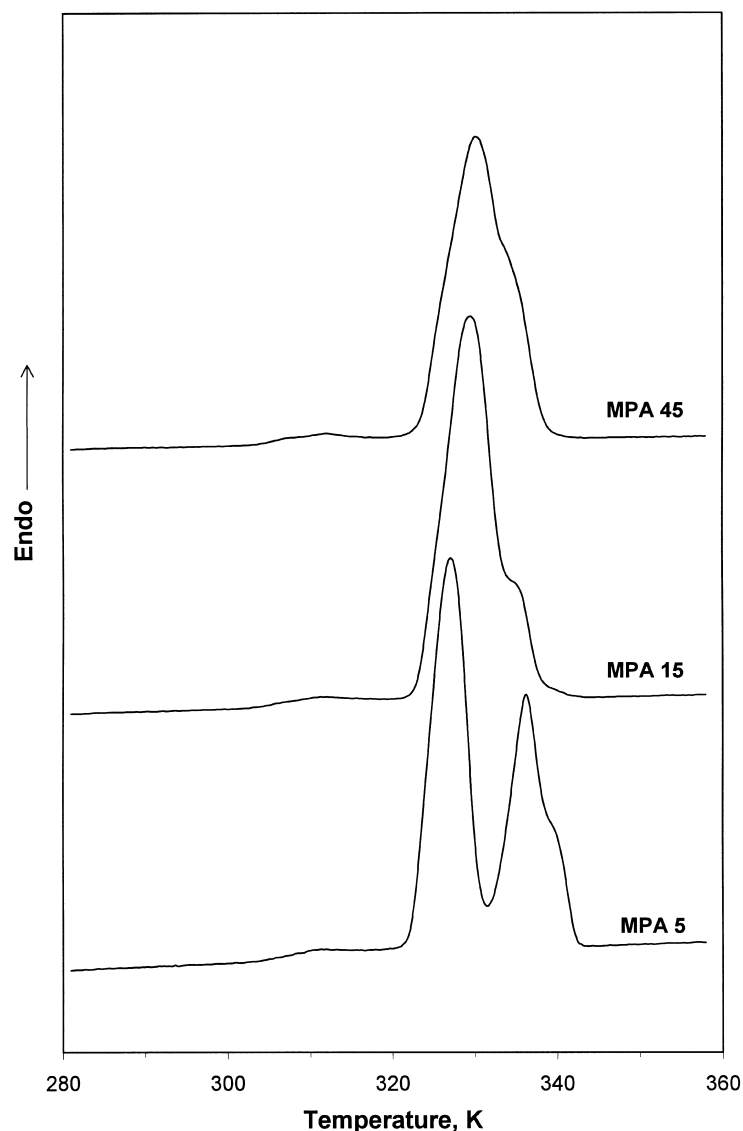


Fig. 2. DSC thermograms of as-prepared samples of MPA. HR = 10 K/min.

non-isothermal crystallization of MPA 5 shows its maximum speed at 250.5 K which is just about 10 K above  $T_g$ . During rescanning in the second run, the thermogram is completely different from that of the as-prepared sample.

For assessment of the exo- and endothermic phenomena taking place during the DSC scan and for estimation of enthalpy of the process, the experimental thermogram of the second run was compared with a hypothetical MPA 5 sample the specific heat of which was changing linearly within the temperature interval 244–336 K (dashed line in the 2nd run curve of Fig. 3). Immediately after the glass transition, the non-isothermal crystallization of the supercooled sample continues which is associated with the exotherm E I (minimum at about 252 K). Another exotherm E II is recorded at about 300 K, followed by two large endotherms III and IV separated by a deep exotherm E III. Of course, it is not possible to evaluate respective

peaks separately but we can make an overall energy balance of the DSC run. The total enthalpic balance of the 2nd run in the temperature interval 244–336 K is +16.9 J/g. This enthalpy corresponds to the crystalline portion present in the sample at the beginning of the 2nd run which was formed during cooling from the melt. Integration of the exotherm on the cooling curve provides, after correction for the heat flow change during the glass transition (see the dashed line on the cooling curve of Fig. 3), the value –16.8 J/g.

Another enthalpic balance can be made separately for the temperature intervals of 244–307 and 307–336 K of the 2nd run curve of Fig. 3. In the first interval, the non-isothermal crystallization started during cooling goes on after passing the  $T_g$  (exotherm E I). Another crystalline portion is formed during additional crystallization characterized by exotherm E II with the minimum at about 300 K. Total enthalpy

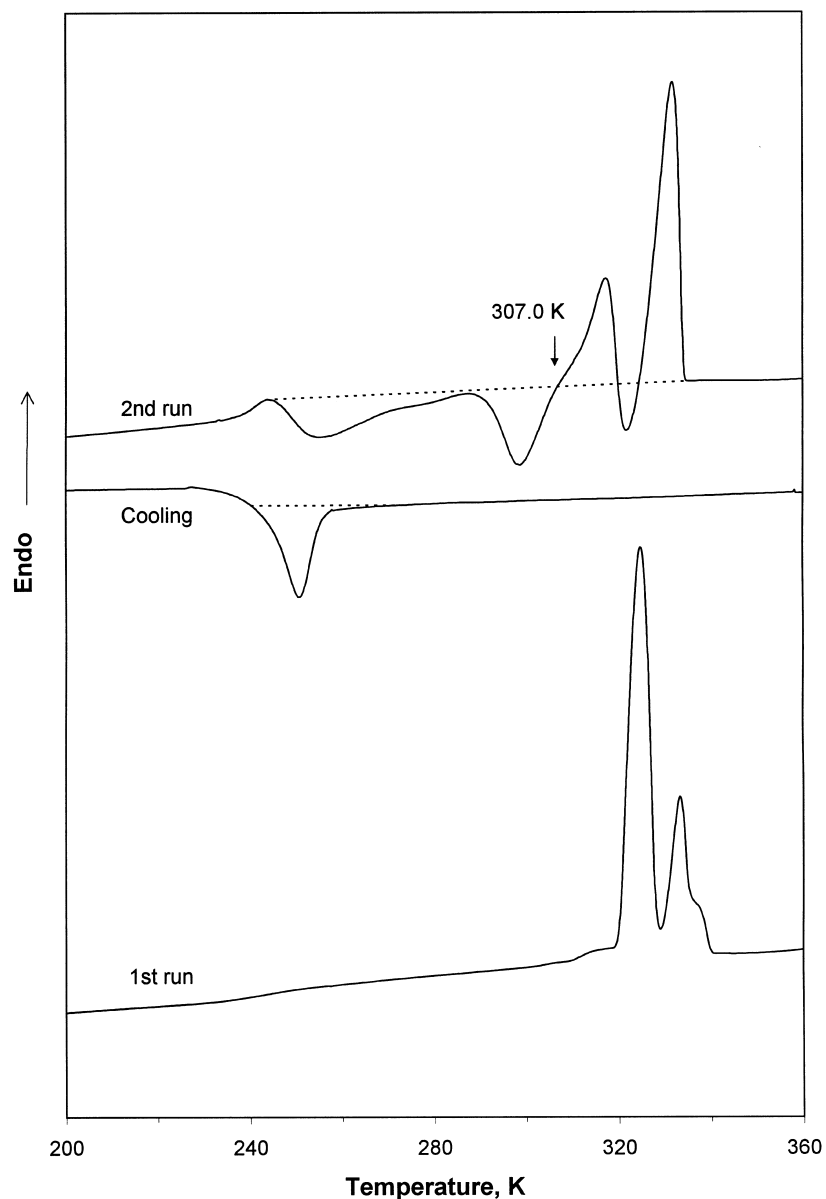


Fig. 3. DSC thermograms of the 1st, 2nd (HR = 10 K/min) and cooling (CR = -10 K/min) runs of as-prepared sample of MPA 5. Dashed lines refer to integration (see the text).

associated with the crystallization during cooling and the subsequent 2nd run up to 307 K is 60.2 J/g. The crystalline portion thus formed melts (endotherm III). This melting is accompanied by recrystallization (exotherm E III, minimum at 324 K) to the final structure melting in the last endotherm IV with the maximum at about 334 K. The net contribution of recrystallization (E III) and subsequent melting (IV) is zero as both these processes take place in the same temperature interval. The total enthalpy in the interval of 307–336 K is 59.0 J/g which is in a reasonably good agreement with the value 60.2 J/g of the first phase of the experiment.

The WAXS diffraction patterns of MPA 15 samples are summarized in Fig. 4. After melting at 360 K for 10 min and rapid quenching to laboratory temperature, the sample is

completely amorphous (Chart A). In the as-prepared sample (Chart B), on the other hand, the crystalline structure is well developed. After subtracting the integral intensity of the amorphous sample, the crystallinity of the as-prepared MPA 15 was estimated at 30%.

In the Raman spectra of all as-prepared partially crystalline samples (Fig. 5), characteristic bands of the amorphous ( $1643$  and  $1079\text{ cm}^{-1}$ ) and crystalline ( $1627\text{ cm}^{-1}$ ) phases [6] are clearly resolved; for MPA15, this is demonstrated in Fig. 5, spectrum B. Using the spectrum of the amorphous phase (Fig. 5, spectrum A) measured at laboratory temperature immediately after cooling down, the sample melted at 360 K; the spectrum of the crystalline component in the as-prepared sample was obtained by subtracting

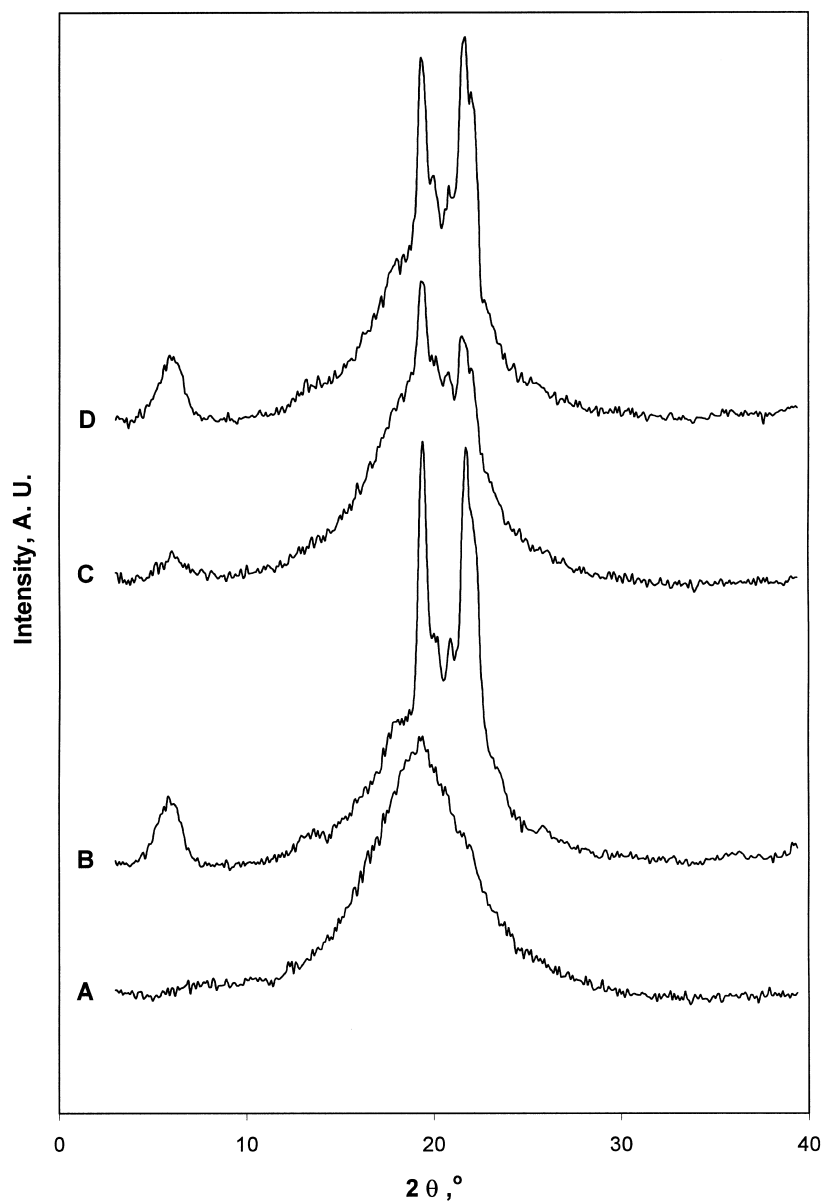


Fig. 4. WAXS patterns of MPA 15 samples: (A) melted at 360 K, quenched; (B) as-prepared; (C and D) crystallized at room temperature (300 K) for 1 and 24 h, respectively.

corresponding normalized spectra (Fig. 3, spectra A and B) so that the intensity of the C=O stretching band at  $1643\text{ cm}^{-1}$  assigned to the amorphous phase [6] was totally suppressed. The subtracting factor  $f$  can be considered a degree of crystallinity, and its values are 46, 38, and 33% for the MPA5, MPA15, and MPA45 samples, respectively. These crystallinities are somewhat higher than those estimated from the WAXS measurements. A possible reason of this fact will be discussed in the second part of this study [15].

### 3.2. Isothermal crystallization at 270 K

Fig. 6 presents DSC thermograms of the MPA 5 samples

crystallized at 270 K for different periods of time. It can be seen that with increasing crystallization time the crystalline portion (endothems III and IV) rises and the scope of additional crystallization (E II) and recrystallization (E III) extends. At temperatures of about  $T_c + 10\text{ K}$ , the thermograms corresponding to crystallization times of 12 min and higher include a flat endotherm I obviously associated with melting of imperfect crystallites formed in the interlamellar space during later stages of the isothermal crystallization. These crystallites are often referred to in literature as “fringed” lamellae and associated with secondary crystallization [16].

The thermograms in Fig. 6 were analysed quantitatively. It follows from the above discussion that in the given

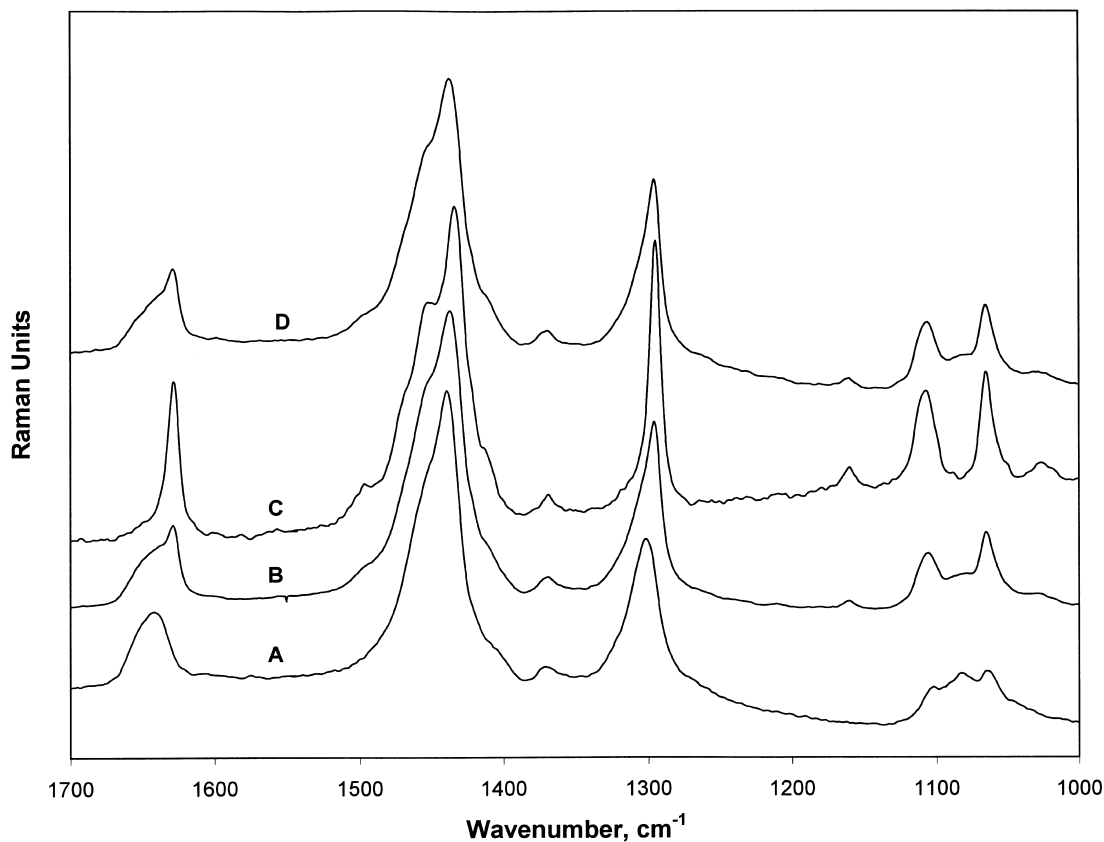


Fig. 5. Raman spectra of MPA15: (A) amorphous, measured at room temperature immediately after cooling down the melted sample (at 360 K for 10 min); (B) as-prepared; (C) difference spectrum  $B - f \times A$  with the subtracting factor  $f = 0.62$  (see the text); (D) isothermally crystallized at room temperature for 48 h.

temperature interval (270–340 K) several parallel and/or consecutive exothermic and endothermic processes are running. For that reason, it is not possible to evaluate quantitatively individual endotherms and exotherms in the thermograms of Fig. 6. Consequently, the integration was performed separately for endotherm I only and the rest of the respective thermogram was integrated as a whole. The results are summarized in Fig. 7.

The typical S-shaped dependences show that the overall isothermal crystallization at 270 K is completed within about 30 min. Endotherm I (curve A) of “fringed” lamellae starts to develop after about 10 min of crystallization, i.e. at the time when formation of the primary crystallites (curve B) has already passed its half-time. Two questions, however, still remain: which endotherm corresponds to the primary lamellae formed during isothermal crystallization and what structure is formed during additional crystallization at about 300 K (exotherm E II). In principle, two structures can be in play here—III and IV.

These problems have been, at least partially, solved by the experiments where different HR of the DSC run were used after isothermal crystallization of the MPA samples. The results are summarized in Fig. 8. The heat flow outputs of respective thermograms were corrected for different HR. At the starting point of the respective DSC runs all samples

were the same, i.e. crystallized at 270 K for 60 min after previous melting.

Endotherm I seems to decrease in its magnitude with decreasing HR. However, this fact is apparently caused by the shape of exotherm II which represents the time-dependent kinetic process of additional crystallization. At low HR this process begins at lower temperatures and the exotherm E II thus partially compensates the endotherm I. With increasing HR, temperature maxima/minima of respective peaks, with the exception of IV, shift towards higher temperatures. This fact is probably associated with thermal inertia of the polymer system and corroborates the kinetic character of the running processes.

A comparison of the curves in Fig. 8 regarding endotherms III and IV shows that the structure formed as primary lamellae during isothermal crystallization at 270 K corresponds to endotherm III and the structure IV is formed in a lesser extent, if any. During the additional crystallization (exotherm E II), the structure formed is apparently also III. The final most perfect structure IV is predominantly formed by recrystallization associated with exotherm E III at about 325 K. At lower HR (curve 2, Fig. 8, in particular) peaks III and E III mutually compensate each other and, as the system has enough time for recrystallization, a large endotherm IV appears in the thermogram. On the other

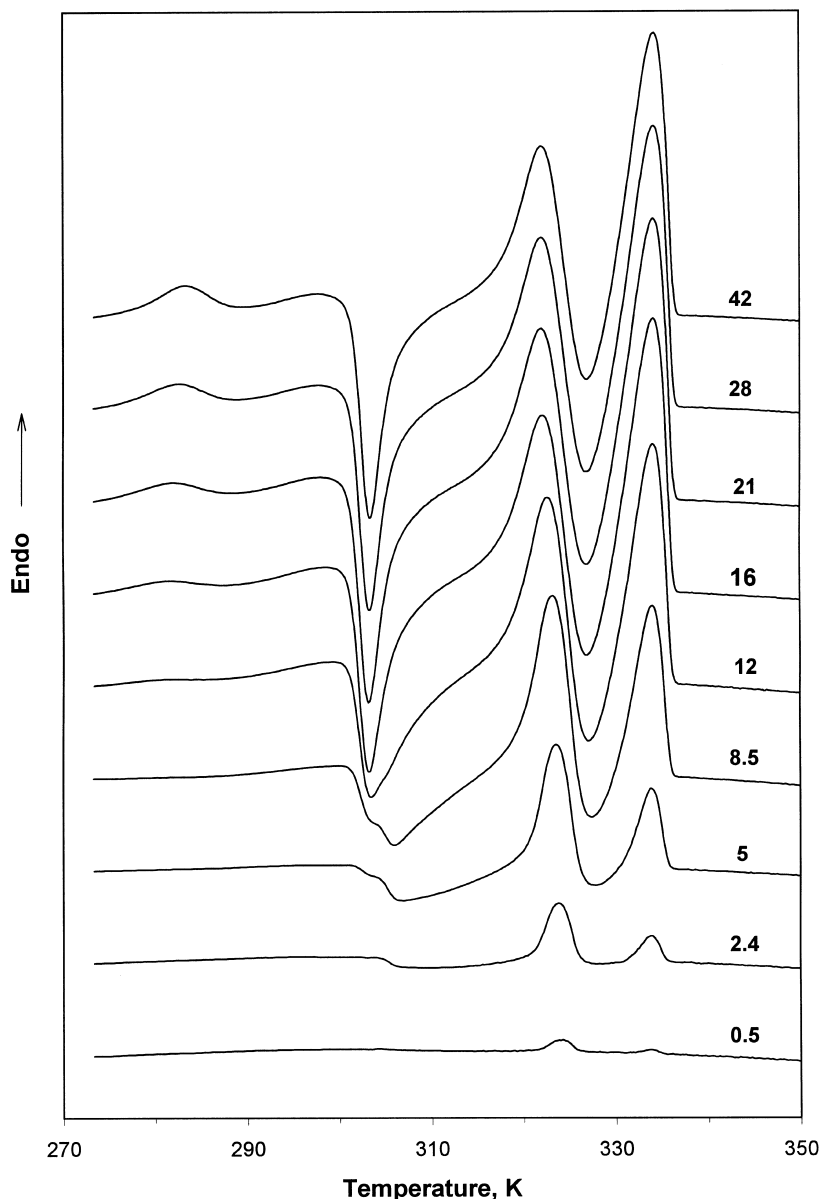


Fig. 6. DSC thermograms of MPA 5 crystallized at 270 K for different periods of time (min) indicated at respective curves. HR = 10 K/min.

hand, at high HR the recrystallization cannot be completed due to the lack of time and endotherm IV almost vanishes in the thermogram 40, Fig. 8.

In the thermograms of HR 20 and 40 K/min in Fig. 8 there is another endotherm II appearing at about 300 K, just before exotherm E II. In the curve of 10 K/min this is expressed as a marked asymmetry of exotherm E II. The endotherm II is probably associated with another low-ordered structure formed in the interlamellar space of the primary lamellae III which differ from the “fringed” lamellae I by a smaller extent of defects. In Fig. 6, the presence of this structure is manifested by a change in the shape of exotherm E II, particularly in curves 5 and 8.5, and, in the curves of longer crystallization times, by a marked asymmetry of exotherm E II. It is, therefore, probable that

during isothermal crystallization at 270 K, the “fringed” interlamellar structure II is formed earlier than the structure I the formation of which starts after about 10 min.

### 3.3. Isothermal crystallization at different temperatures

The DSC thermograms of MPA 5 samples crystallized at respective crystallization temperatures  $T_c$  within the range of 250–305 K for 60 min are shown in Fig. 9. One can easily detect that there is a marked difference in the thermograms corresponding to the crystallization temperatures  $T_c = 250 - 280$  K and those for  $T_c = 290$  K and higher.

All thermograms begin with a small endotherm I of “fringed” lamellae, the maximum of which appears at about  $T_c + 10$  K. In the thermograms for  $T_c = 250$  and



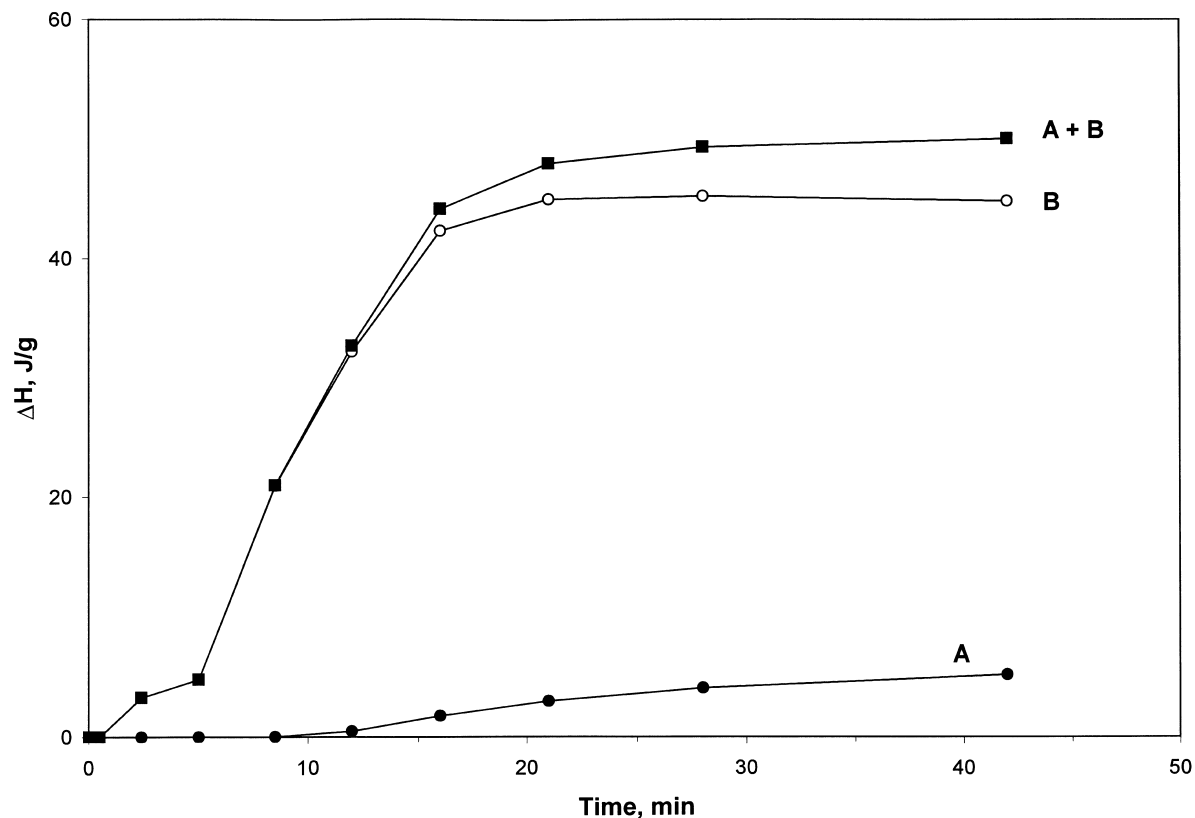


Fig. 7. Enthalpic balance of thermograms from Fig. 6: (A) peak I (see Fig. 1); (B) rest of the thermogram (from the point just after peak I to 340 K).

260 K there is a hint of exotherm E I just after endotherm I. This exotherm E I is associated with non-isothermal crystallization facilitated by increased mobility of polymer chains as they are heated from the supercooled state.

In the thermograms of  $T_c$  up to 280 K there is a pronounced exotherm E II with minimum at about 300 K. It is associated with additional crystallization with predominant formation of the structure III. This structure subsequently recrystallizes (exotherm E III at about 326 K) to the final structure IV. Small endotherm appearing on the curve of  $T_c = 280$  K at about 305 K corresponds probably to the less-defected “fringed” lamellae II discussed above with Figs. 6 and 8.

In the thermograms corresponding to  $T_c$  of 290 K and higher, exotherm E II is no longer present which means that during isothermal crystallization at these  $T_c$ , the structure III is directly formed in a single step. At 305 K the crystallization is already very slow which results in tiny endotherms in the pertaining thermogram.

The maximum of endotherm I, corresponding to melting of the imperfect crystallites formed in later stages of isothermal crystallization at respective  $T_c$ , shows a strong dependence on  $T_c$ . As crystallization during the DSC scan proceeds, the temperature of endotherm III ( $T_m$  316–320 K) becomes less dependent on  $T_c$  until, finally, the highest-melting endotherm IV shows almost a negligible dependence on the original crystallization temperature. This is

obviously a consequence of the fact that the crystalline structure IV associated with this endotherm was not formed at the given  $T_c$  but by recrystallization from the structure III during the DSC scan.

The thermograms in Fig. 9 were quantitatively evaluated with respect to their overall enthalpy balance. Integration limits were the point just before endotherm I and the final baseline point after endotherm IV. The results in J/g thus correspond to the degree of crystallinity of the samples isothermally crystallized at the respective  $T_c$  for 60 min. The results are shown in Fig. 10.

In the range of  $T_c = 250$ –280 the dependence has a monotonous decreasing trend as it is usually found in polymer systems [17]. However, the crystallinity at  $T_c = 290$  K shows a jump-like upward deviation from this trend. In Fig. 9, this corresponds to the first thermogram (as ordered according to increasing  $T_c$ ) where exotherm E II is not present and the structure III is formed in a single isothermal step.

This jump-like change in crystallization behaviour can probably be associated with a conformational transition on the C–N bond of MPA discussed by Shalaby [5]. As it is shown on the cooling thermogram in Fig. 3, no crystallization takes place in this temperature region during cooling. The non-isothermal crystallization on cooling from the melt begins at substantially greater supercoolings just above  $T_g$ . The mentioned conformational transition

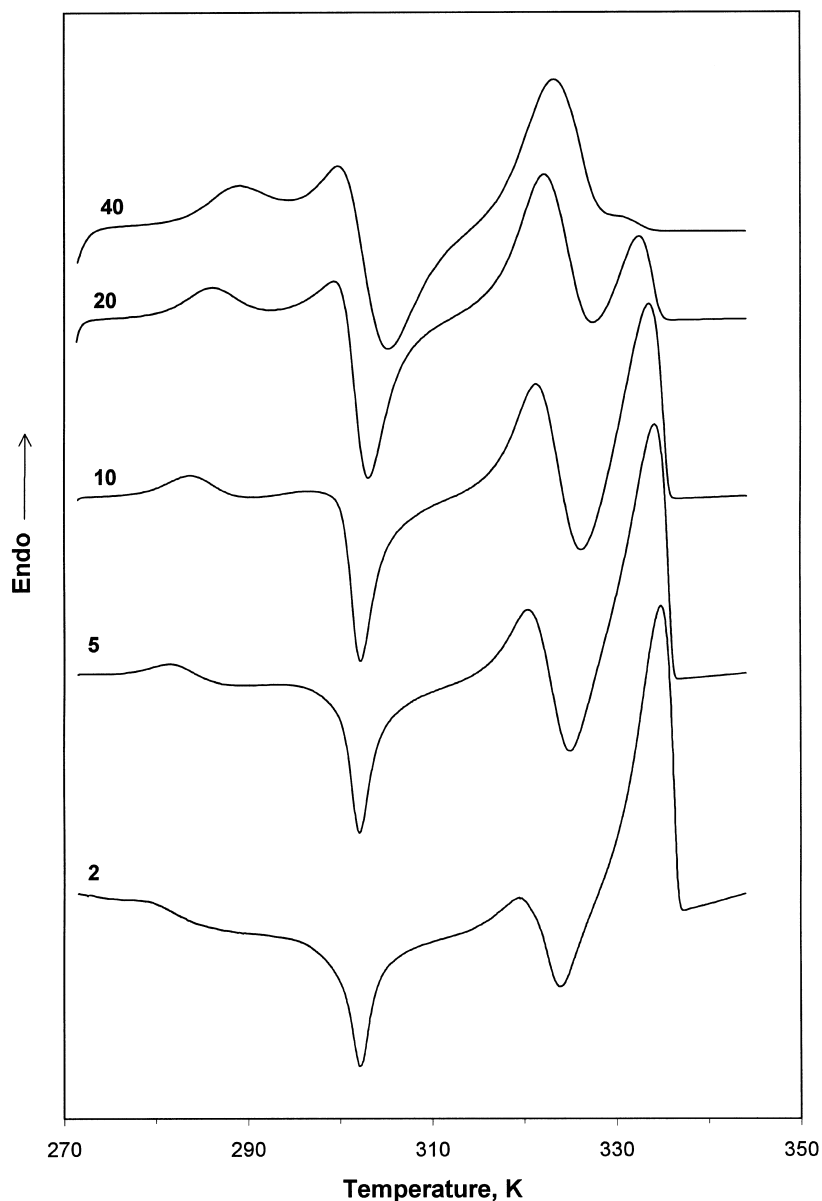


Fig. 8. DSC thermograms of MPA 5 crystallized at 270 K for 60 min scanned at different HR (K/min) indicated at respective curves.

probably facilitates, after a certain induction period, formation of a larger number of nucleation centres at 290 K than at lower temperatures. This results in a dramatic increase in crystallinity of the sample with  $T_c$  of 290 K. This conformational transition is probably also a reason for the existence of exotherm E II of additional crystallization on thermograms of the MPA samples isothermally crystallized at  $T_c$  up to 280 K (Fig. 9). This problem is discussed in detail in the second part of the present study [15].

The results of isothermal crystallization at 270 K and at different  $T_c$  have been shown for the sample MPA 5 only. The samples MPA 15 and MPA 45 provided similar results. However, a higher molecular weight and therewith associated higher viscosity of the melt slows down the crystallization process in these samples and, consequently,

the respective peaks in the thermograms are less well separated.

### 3.4. Long-term crystallization at 300 K

The crystallization process in MPA was also studied as a function of time within an interval of up to one month. Fig. 11 shows the DSC thermograms of MPA 15 samples crystallized at 300 K (laboratory temperature) for different periods of time. As it has been discussed above (Fig. 9), the two-step crystallization, i.e. isothermal crystallization at respective  $T_c$  and additional crystallization during the DSC scan at about 300 K (exotherm E II), combines into a single step at  $T_c = 290$  K and higher. In Fig. 11, the ordered structure III thus formed is represented by the

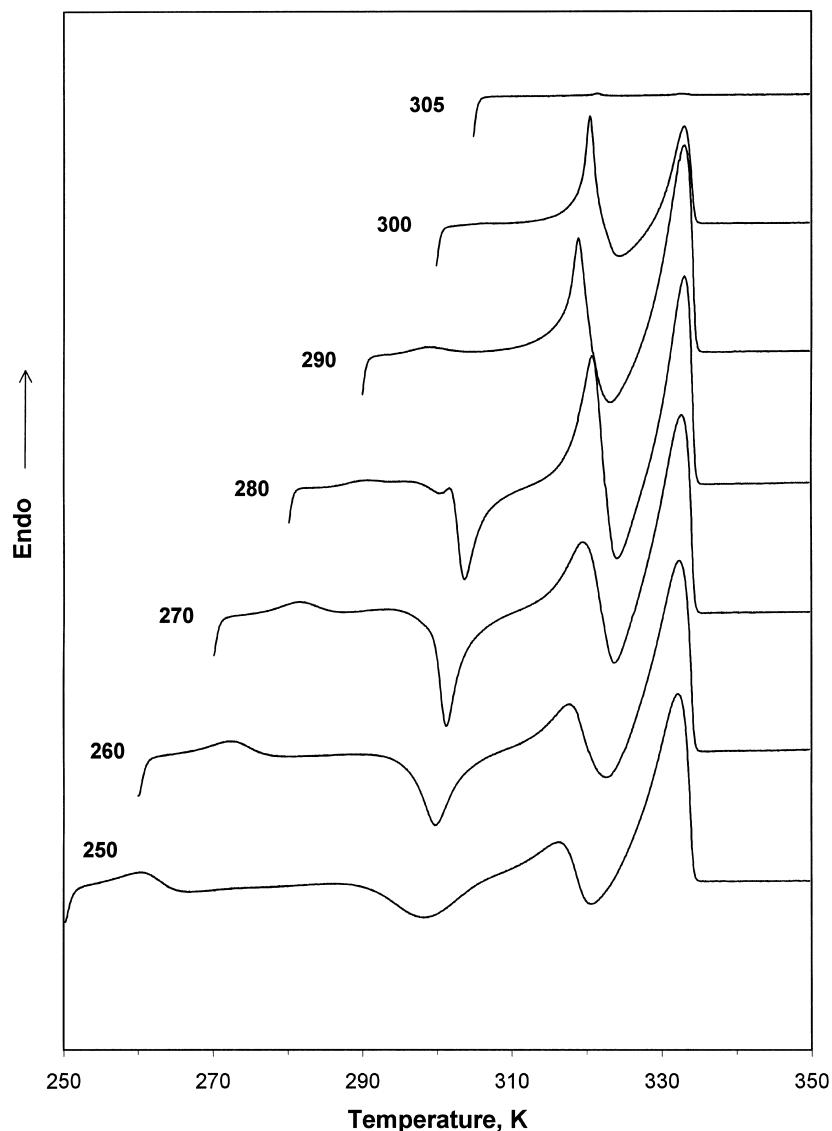


Fig. 9. DSC thermograms of MPA 5 samples crystallized at respective crystallization temperatures (K) for 60 min. HR = 5 K/min.

melting endotherm at 324.5 K. Its maximum is virtually independent of time, which implies that from the early stages of crystallization the crystalline structure III is organized into the same degree of perfection and just the amount of this phase increases with time.

As in all previous cases, the ordered structure III undergoes recrystallization associated with exotherm E III at about 328 K. The resulting final, higher-ordered crystalline structure IV shows melting endotherm at about 336 K the maximum of which very slightly increases with the crystallization time.

As crystallization proceeds, an additional lower-melting endotherm appears at about 308–309 K (i.e. approximately at  $T_c + 10$  K), which corresponds to the less-ordered structure I of “fringed” lamellae formed during later stages of the long-term crystallization.

The overall enthalpy balances of the thermograms of the

sample MPA 15 crystallized at 300 K for 60 min and one month are 11.3 and 57.9 J/g, respectively, as compared with the value 23.5 J/g for the MPA 5 sample crystallized at 300 K for 60 min.

Fig. 4 presents WAXS diffraction patterns of the amorphous (after melting at 360 K) MPA 15 sample (chart A) and of the same samples crystallized at laboratory temperature for 1 and 24 h (charts C and D). A comparison of the WAXS curves of crystallized samples indicates the same crystalline modification. Quantitative evaluation of the WAXS diffraction patterns (Fig. 12) shows that crystallinity of the MPA 15 sample reaches asymptotically about 34% within 24 to 30 h. Fig. 12 also shows crystallinities of MPA 15 determined by Raman spectroscopy. These results are in the asymptote somewhat higher than those obtained by WAXS measurements. A possible reason is discussed in the second part of the present study [15].

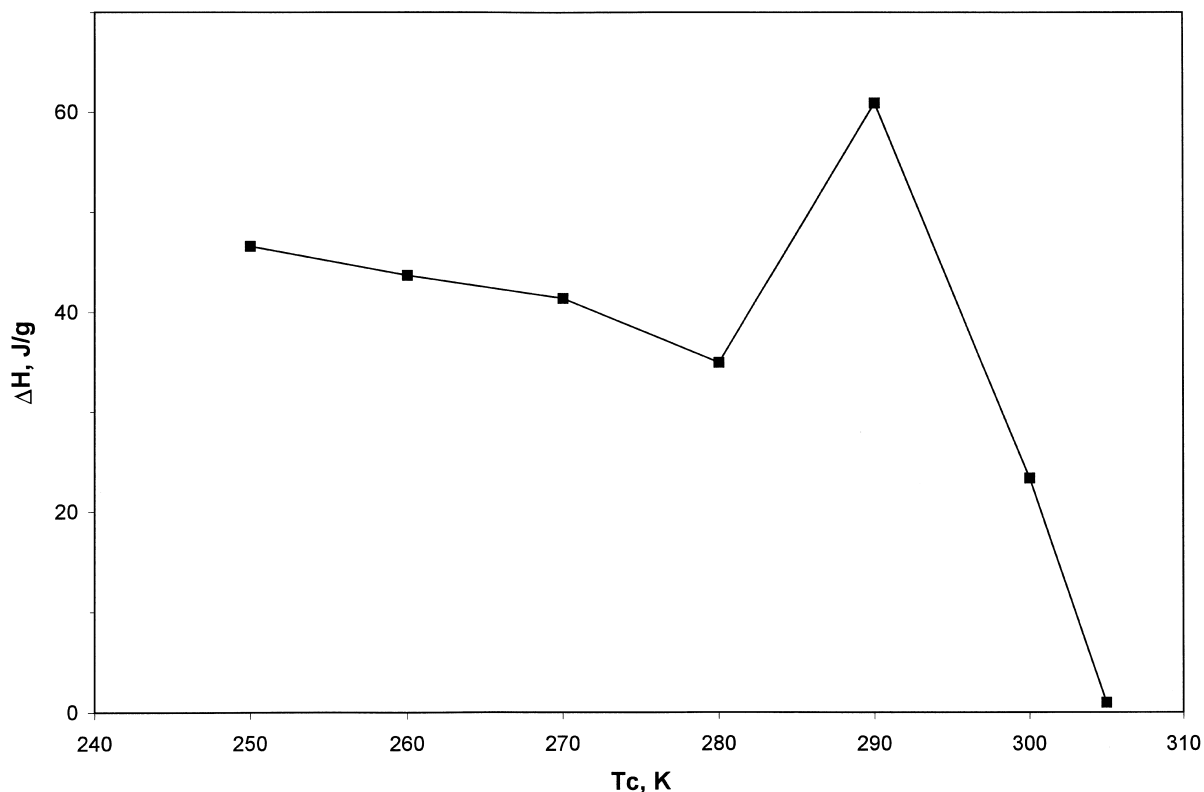


Fig. 10. Overall enthalpic balance of thermograms from Fig. 9.

#### 4. Conclusions

The calorimetric (DSC), X-ray (WAXS) and spectroscopic (Raman) studies have revealed a complex melting/crystallization behaviour of MPA. On the DSC thermograms of two as-prepared higher molecular weight samples (MPA 15 and MPA 45), the main endotherm at 330 K is accompanied by a shoulder peak at 335 K. In the low-molecular weight sample (MPA 5), these two endotherms are almost completely separated and show maxima at 327 and 336 K, respectively. The degrees of crystallinity of the as-prepared samples are 30% for MPA 15 (WAXS) and 46, 38 and 33% for MPA 5, 15 and 45, respectively (Raman).

In systems where several parallel and/or consecutive exo- and endothermic processes are running, it is not possible to quantitatively evaluate individual DSC peaks. For a semi-quantitative assessment of the processes, however, an overall enthalpic balance of a DSC run can be used. The exotherm of non-isothermal crystallization recorded on cooling the MPA 5 sample from the melt provided, after correction for glass transition, the same value of enthalpy as the overall enthalpic balance of the subsequent second DSC run.

The DSC runs of MPA 5 samples isothermally crystallized at 270 K for different periods of time have shown that formation of primary lamellae III melting at about 324 K is

completed within 30 min. After about 10 min of isothermal crystallization, formation of the less-ordered “fringed” lamellae I melting at about  $T_c + 10$  K begins. This structure is often attributed to secondary crystallization in the inter-lamellar space of primary lamellae. During heating in the DSC run, a pronounced exotherm E II appears at about 300 K which is associated with additional crystallization of the form III. On further heating, this structure undergoes recrystallization associated with a marked exotherm E III at about 327 K. The resulting more perfect final structure IV melts at about 335 K.

The DSC experiments carried out at different HR with the MPA 5 sample crystallized at 270 K for 60 min have corroborated the hypothesis that the structure III is formed as primary lamellae during isothermal crystallization and also by additional crystallization during the DSC scan. The final most perfect structure IV is predominantly formed by recrystallization of the structure III on heating.

Some DSC thermograms also show another small endotherm II just at the edge of exotherm E II which probably corresponds to less-defected “fringed” lamellae formed in the system earlier than structure I.

The DSC experiments carried out on the samples isothermally crystallized at different  $T_c$  (250–305 K) have shown a marked difference between the thermograms corresponding to  $T_c = 250 - 280$  K and 290–305 K. At lower  $T_c$ , the primary structure III crystallizes in two steps, the second

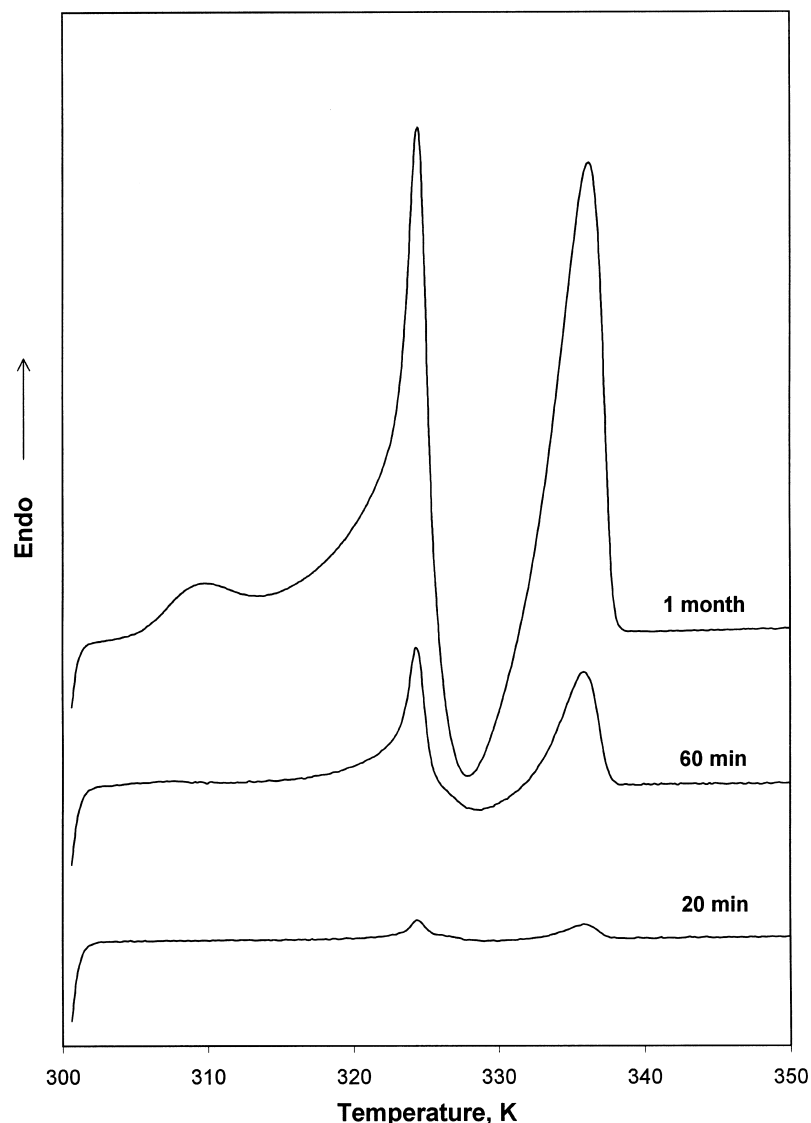


Fig. 11. DSC thermograms of MPA 15 after isothermal crystallization at 300 K for 20, 60 min and 1 month.

taking place during the DSC run as additional crystallization with the maximum speed at about 300 K. At  $T_c = 290$  K and higher, the primary structure III is directly formed in a single isothermal crystallization step.

The temperature maximum of endotherm I corresponding to melting of the crystallites formed during later stages of isothermal crystallization shows a strong dependence on  $T_c$ . The maximum of endotherm III of primary crystallization lamellae is less dependent on  $T_c$ . Finally, the highest-melting endotherm IV shows almost a negligible dependence on the original crystallization temperature. This reflects the fact that the final crystalline structure is not formed at a given  $T_c$  but by recrystallization of the structure III.

The dependence of crystallinity of the MPA samples isothermally crystallized at  $T_c = 250 - 305$  K on crystallization temperature has a decreasing trend with a

jump-like upward deviation at 290 K. This sudden increase in crystallinity might be attributed to a conformational transition on the C–N bond of MPA. This transition probably facilitates formation of a larger number of nucleation centres leading to a dramatic increase in crystallinity. Here we can also search for a reason of additional crystallization of the structure III on heating after isothermal crystallization at a  $T_c$  up to 280 K.

The long-term crystallization (at 300 K) DSC thermograms show the main endotherm III of primary lamellae melting at 324.5 K and final melting endotherm IV of the recrystallized structure at 336 K. The minor endotherm I of imperfect “fringed” crystallites occurs at 309 K during later stages of crystallization. Within 24–30 h, the crystallinity of MPA 15 reaches asymptotically about 34% (WAXS).

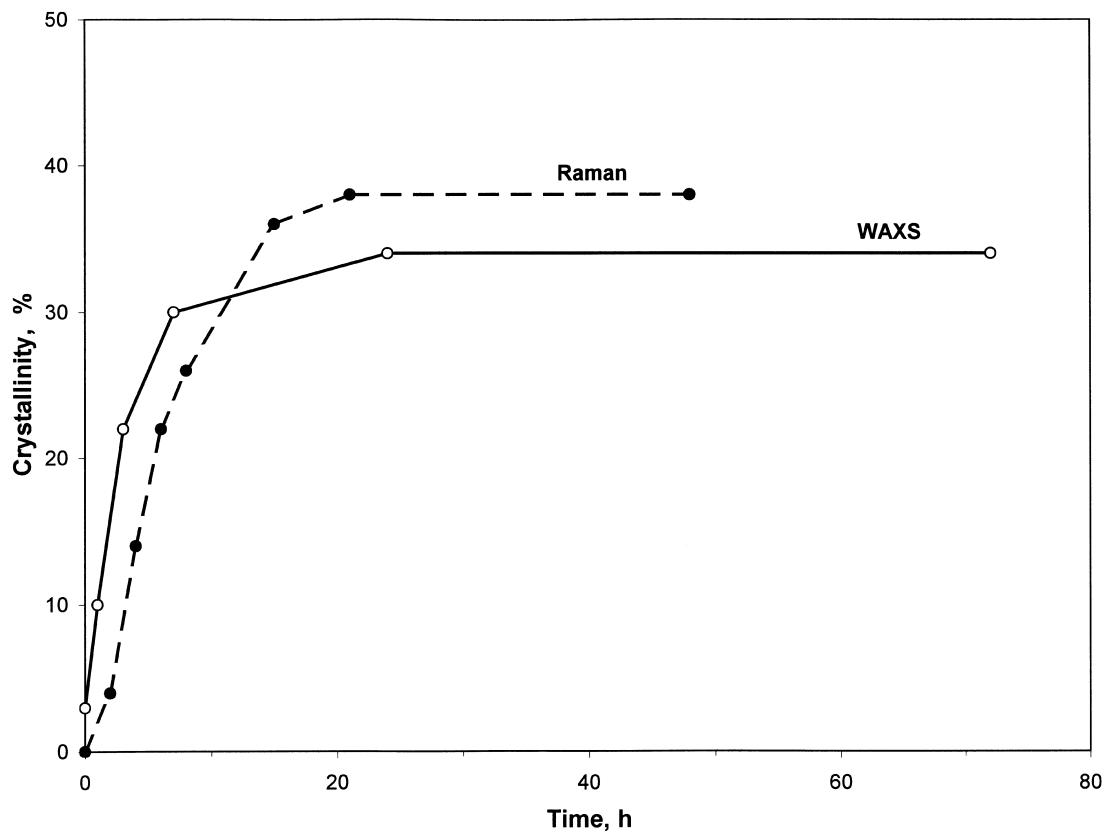


Fig. 12. Time dependence of crystallinity of MPA 15 at 300 K determined by WAXS and Raman spectroscopy.

### Acknowledgements

The authors would like to express their thanks to the Grant Agency of the Academy of Sciences of the Czech Republic (Grant no A4050605) and the Grant Agency of the Czech Republic (Grant no 203/97/0539) for financial support.

### References

- [1] Briggs BS, Frosch CJ, Erickson RH. *Ind Eng Chem* 1946;38:1016.
- [2] Wittbecker EL, Houtz RC, Watkins WW. *Ind Eng Chem* 1948;40: 875.
- [3] Shalaby SW, Fredericks RJ, Pearce EM. *J Polym Sci: Part A2* 1972; 10:1699.
- [4] Shalaby SW, Fredericks RJ, Pearce EM. *J Polym Sci: Part B: Polym Phys* 1973;11:939.
- [5] Shalaby SW, Fredericks RJ, Pearce EM. *J Polym Sci: Part B: Polym Phys* 1974;12:223.
- [6] Schmidt P, Straka J, Dybal J, Schneider B, Doskočilová D, Puffr R. *Polymer* 1995;36:4011–21.
- [7] Bassett DC, Olley RH, Al Raheil IAM. *Polymer* 1988;29:1745.
- [8] Woo EM, Ko TY. *Colloid Polym Sci* 1996;274:309.
- [9] Chen CY, Woo EM. *Polym J* 1995;27:361.
- [10] Muellerleile JT, Risch BG, Rodriguez DE, Wilkes GL. *Polymer* 1993; 34:789.
- [11] Rodriguez-Arnold J, Zhang A, Cheng SZD, Lovinger AJ. *Polymer* 1994;35:1884.
- [12] Ji XL, Zhang WJ, Wu ZW. *J Polym Sci: Part B: Polym Phys* 1997; 35:431.
- [13] Petrillo E, Russo R, D'Aniello C, Vittoria V. *J Macromol Sci Phys* 1998;B37:15.
- [14] Puffr R, Tuzar Z, Mrkvičková L, Šebenda J. *Makromol Chem* 1983;184:1957.
- [15] Kratochvíl J, Sikora A, Baldrian J, Dybal J, Puffr R. *Polymer* 2000;41:7667.
- [16] Marand H, Alizadeh A. *Polym Mater Sci Eng* 1999;81:238.
- [17] Mandelkern L. *Crystallization of polymers*. New York: McGraw-Hill, 1964.